Langmuir
Article
pubs.acs.org/Langmuir

Attachment of L-Glutamate to Rutile (α-TiO_2): A Potentiometric, Adsorption, and Surface Complexation Study

Caroline M. Jonsson,*[,†,‡] Christopher L. Jonsson,[†,‡] Dimitri A. Sverjensky,[†,‡] Henderson J. Cleaves,[‡] and Robert M. Hazen[‡]

[†]*Department of Earth & Planetary Sciences, Johns Hopkins University, Baltimore, Maryland 21218, and* [‡]*Geophysical Laboratory, Carnegie Institution of Washington, 5251 Broad Branch Road NW, Washington, D.C. 20015*

Received May 7, 2009. Revised Manuscript Received June 17, 2009

Interactions between aqueous amino acids and mineral surfaces influence the bioavailability of amino acids in the environment, the viability of Ti implants in humans, and the role of mineral surfaces in the origin of life on Earth. We studied the adsorption of L-glutamate on the surface of rutile (α-TiO_2, pH_{PZC} = 5.4) in NaCl solutions using potentiometric titrations and batch adsorption experiments over a wide range of pH values, ligand-to-solid ratios, and ionic strengths. Between pH 3 and 5, glutamate adsorbs strongly, up to 1.4 μmol m^{-2}, and the adsorption decreases with increasing ionic strength. Potentiometric titration measurements of proton consumption for the combined glutamate−rutile−aqueous solution system show a strong dependence on glutamate concentration. An extended triple-layer surface complexation model of all the experimental results required at least two reaction stoichiometries for glutamate adsorption, indicating the possible existence of at least two surface glutamate complexes. A possible mode of glutamate attachment involves a bridging-bidentate species binding through both carboxyl groups, which can be thought of as "lying down" on the surface (as found previously for amorphous titanium dioxide and hydrous ferric oxide). Another involves a chelating species which binds only through the γ-carboxyl group, that is, "standing up" at the surface. The calculated proportions of these two surface glutamate species vary strongly, particularly with pH and glutamate concentration. Overall, our results serve as a basis for a better quantitative understanding of how and under what conditions acidic amino acids bind to oxide mineral surfaces.

1. Introduction

Interactions of aqueous organic molecules with a variety of functional groups, such as amino acids, with the hydroxylated surface sites on metal oxide minerals are of fundamental interest in a wide range of disciplines.[1] These interactions may influence the degradation, mobility, and bioavailability of amino acids in the environment. In addition, interactions between aqueous amino acids and oxide surfaces govern the viability of metal implants in the human body and may have played an important role in the origin of life on Earth. The adsorption behavior and speciation of amino acids are strongly influenced by environmental conditions such as pH, salinity, and total concentration of amino acids and mineral particles.[1] The present study is focused on the amino acid L-glutamic acid and its adsorption onto nanosized rutile (α-TiO_2) particles. Glutamate is a polar molecule with three proton-active groups: an amine group and two carboxyl groups.[2] Although previous studies showed that glutamate adsorbs to hydrous ferric oxide,[3,4] titanium dioxide,[5−7] aluminum hydroxides,[8−10] and silica,[11,12] there are no studies in the literature on the adsorption of glutamate to mineral surfaces covering a wide range of environmental conditions.

In our work, the mineral rutile was chosen for several reasons. In order to understand the chemistry at the mineral−water interface at a molecular level, it is necessary to use a well-characterized mineral surface. Rutile surface chemistry can be studied over a wide pH range and a number of thorough previous experimental and theoretical studies have established that it is a model colloidal oxide.[13−19] Rutile is a particularly useful oxide to study because it has a high dielectric constant that results in the highest equilibrium adsorption constants for all oxides. Experimental equilibrium constants for rutile can therefore be readily extrapolated to other oxides with lower dielectric constants using Born solvation theory.[20−22]

*Corresponding Author: Tel. 1-202-478-8915. Fax: 1-202-478-8901. E-mail: cjonsson@ciw.edu.

(1) Lambert, J. F. *Origins Life Evol. Biospheres* **2008**, *38*, 211–242.
(2) Waelsch, H. *Methods Enzymol.* **1957**, *3*, 570–575.
(3) Davis, J. A.; Leckie, J. O. *Environ. Sci. Technol.* **1978**, *12*, 1309–1315.
(4) Sverjensky, D. A.; Jonsson, C. M.; Jonsson, C. L.; Cleaves, H. J.; Hazen, R. M. *Environ. Sci. Technol.* **2008**, *42*, 6034–6039.
(5) Roddick-Lanzilotta, A. D.; McQuillan, A. J. *J. Colloid Interface Sci.* **2000**, *227*, 48–54.
(6) Tentorio, A.; Canova, L. *Colloids Surf.* **1989**, *39*, 311–319.
(7) Fuerstenau, D. W.; Chander, S.; Lin, J.; Parfitt, G. D. *ACS Symp. Ser.* **1984**, *253*, 311–327.
(8) Fitts, J. P.; Persson, P.; Brown, G. E., Jr.; Parks, G. A. *J. Colloid Interface Sci.* **1999**, *220*, 133–147.
(9) Moitra, S.; Mundhara, G. L.; Tiwari, J. S. *Colloids Surf.* **1989**, *41*, 311–326.
(10) Micera, G.; Erre, L. S.; Dallocchio, R. *Colloids Surf.* **1987**, *28*, 147–157.
(11) Basiuk, V. A.; Gromovoy, T. Y. *Colloid Surf. A-Physicochem. Eng. Asp.* **1996**, *118*, 127–140.
(12) Churchill, H.; Teng, H.; Hazen, R. M. *Am. Mineral.* **2004**, *89*, 1048–1055.
(13) Fedkin, M. V.; Zhou, X. Y. Y.; Kubicki, J. D.; Bandura, A. V.; Lvov, S. N.; Machesky, M. L.; Wesolowski, D. J. *Langmuir* **2003**, *19*, 3797–3804.
(14) Machesky, M. L.; Wesolowski, D. J.; Palmer, D. A.; Ichiro-Hayashi, K. *J. Colloid Interface Sci.* **1998**, *200*, 298–309.
(15) Ridley, M. K.; Machesky, M. L.; Palmer, D. A.; Wesolowski, D. J. *Colloid Surf. A-Physicochem. Eng. Asp.* **2002**, *204*, 295–308.
(16) Zhang, Z.; Fenter, P.; Cheng, L.; Sturchio, N. C.; Bedzyk, M. J.; Predota, M.; Bandura, A.; Kubicki, J. D.; Lvov, S. N.; Cummings, P. T.; Chialvo, A. A.; Ridley, M. K.; Benezeth, P.; Anovitz, L.; Palmer, D. A.; Machesky, M. L.; Wesolowski, D. J. *Langmuir* **2004**, *20*, 4954–4969.
(17) Panagiotou, G. D.; Petsi, T.; Bourikas, K.; Garoufalis, C. S.; Tsevis, A.; Spanos, N.; Kordulis, C.; Lycourghiotis, A. *Adv. Colloid Interface Sci.* **2008**, *142*, 20–42.
(18) Ziemniak, S. E.; Jones, M. E.; Combs, K. E. S. *J. Solution Chem.* **1993**, *22*, 601–623.
(19) Pang, C. L.; Lindsay, R.; Thornton, G. *Chem. Soc. Rev.* **2008**, *37*, 2328–2353.
(20) Sverjensky, D. A. *Geochim. Cosmochim. Acta* **2005**, *69*, 225–257.
(21) Sverjensky, D. A. *Geochim. Cosmochim. Acta* **2006**, *70*, 2427–2453.
(22) Sverjensky, D. A.; Fukushi, K. *Geochim. Cosmochim. Acta* **2006**, *70*, 3778–3802.

Furthermore, rutile was probably present on prebiotic Earth,[23] which makes amino acid interactions with rutile interesting for origin of life studies. Finally, the adsorption of glutamate and aspartate on amorphous titanium dioxide has been intensively studied using ATR-FTIR spectroscopy,[5] resulting in the inference that several surface species could be present simultaneously: a bridging-bidentate complex involving four points of attachment of glutamate to the surface, a chelating-monodentate complex involving three points of attachment, and a chelating complex involving two points of attachment.[4] Theoretical molecular calculations of glutamate adsorption, however, showed only weak binding to the rutile (100) surface but much stronger binding to the anatase (101) surface.[24]

The overall aim of our research is to obtain a fundamental understanding of the speciation and coordination chemistry of glutamate and other amino acids on the surface of rutile under varying environmental conditions. As a first step, we have performed an extensive study of L-glutamic acid interactions with rutile as a function of pH, ionic strength, and ligand-to-solid ratio using potentiometric titrations and batch adsorption experiments. The present paper is focused on quantitative experimental data integrated with a newly developed surface complexation model. In a parallel study, we are performing ATR-FTIR spectroscopic measurements and theoretical molecular calculations on this system. To our knowledge, this is the first comprehensive study of amino acid interactions with minerals in electrolyte solutions.

2. Materials and Methods

2.1. Materials. All solutions and suspensions were made from Milli-Q water (Millipore, resistance = 18.2 MΩ cm^{-1}), and NaCl (Fisher BioReagents p.a., dried at 180 °C) was used to provide a constant ionic medium of 0.01−0.3 M Na(Cl). The parentheses around Cl^- indicate that the chloride concentration was allowed to vary, while the sodium ion concentration was held constant. Stock solutions of HCl (J.T. Baker, p.a.) were standardized against tris(hydroxymethyl)aminomethane (Trizma base, Fisher Scientific 99.9%). NaOH (J.T. Baker) solutions were standardized against these standardized HCl solutions. L-Glutamic acid (Acros Organics, 99%) was used without further purification. For amino acid analysis, the following chemicals were used without further treatment: ninhydrin (Aldrich, 97%), 2-methoxyethanol (Sigma-Aldrich, 99.9%), acetic acid (Sigma-Aldrich, 99%), sodium acetate (Sigma-Aldrich, 99%), NaCN (Fisher), and ethanol (The Warner Graham Company, 200 proof).

The rutile powder used in the present work was obtained from Oak Ridge National Laboratory (courtesy of J. Rosenqvist, D. Wesolowski, and M. Machesky). At Oak Ridge National Laboratory, rutile powder from Tioxide Specialties Ltd. (Cleveland, UK) was pretreated using the procedure developed by Machesky et al.[14] The powder was first subjected to numerous washing−boiling−decanting cycles in Milli-Q water, then further washed with Milli-Q water until the supernatant had a pH > 4. The solids were then resuspended in fresh Milli-Q water, the suspension placed in a Teflon-lined autoclave, and thermally treated at ∼200 °C for two weeks. The acid released during the thermal treatment was removed by repeated washing−decanting cycles, the suspension thermally treated for three days at ∼200 °C and purified by further washing-decanting cycles, until the pH of the supernatant was above 5. The powder was then dried in a vacuum oven at ∼60 °C. A specific surface area of 18.1 ± 0.1 $m^2 g^{-1}$ was determined using the BET N_2 adsorption method.[25] X-ray powder diffraction (XRD) was used in our laboratory to confirm that the resulting particles were rutile, and scanning electron microscopy (SEM) (Figure 1) showed that the particles are needle shaped, approximately 50−100 nm wide and 400−500 nm long. The predominant growth face is (110). The crystal-termination faces appear to be (101) and (111). The extent to which these faces may be present as steps on the (110) face is not known.

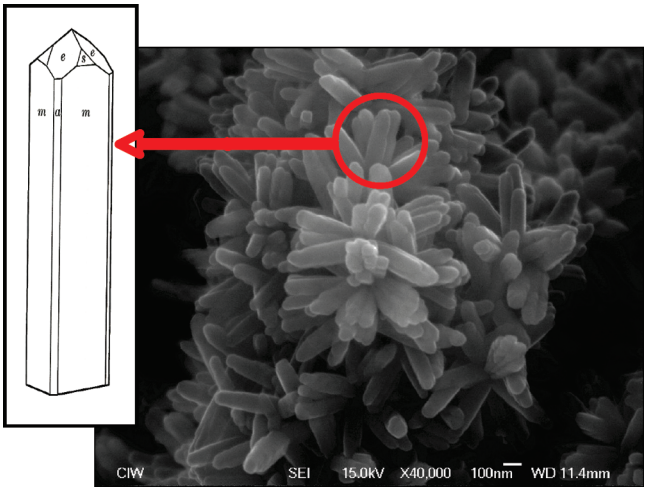

Figure 1. SEM image of the rutile powder used in this work. The sketch on the left-hand side was modified from Dana et al.[26] The principal (110) rutile prismatic crystal faces are labeled "m". Minor (100), (101), and (111) faces are labeled "a", "e", and "s", respectively.

2.2. Experimental Methods. *2.2.1. Potentiometric Titrations.* Automated potentiometric titrations were performed to investigate the (de)protonation reactions of soluble glutamate species, as well as the surface of rutile in the absence and presence of glutamate, using a titrator (Metrohm 836 Titrando) equipped with two dosimeters (800 Dosino) and a combination electrode (Metrohm Ecotrode Plus) calibrated with standardized pH buffers (Fisher Scientific). The H^+-glutamate and H^+-rutile systems were studied at two constant ionic media of 0.01 and 0.1 M Na(Cl), respectively, while the ionic medium in the H^+-glutamate-rutile system was 0.1 M Na(Cl). The temperature of the test solution/suspension was kept constant at 25.0 ± 0.1 °C by the continuous flow of water surrounding the titration vessel, controlled by a thermostatic water bath (Lauda RE104). In order to avoid contamination from $CO_2(g)$ from the air, an inert atmosphere was established in the closed titration vessel by using continuous flow of Ar(g). Stable potentials within ±0.1 mV were usually reached within 10−30 min after each addition of acid or base, and the equilibria were found to be reversible.

Because of previous reports[27−29] of photocatalytic effects of TiO_2 on the degradation of various organic substrates, we performed selected titrations of the combined glutamate−rutile system in darkness by covering the titration vessel with aluminum foil. However, data from dark titrations turned out to be identical to titrations without cover and it was therefore assumed that indoor laboratory lights do not affect this chemical system.

Potentiometric titration data are visualized in plots showing net acid added per mole of glutamate (m_H) in the H^+-glutamate system according to eq 1:

$$m_H = \frac{([H]_{added} - \{H^+\}_{aq}) - ([OH]_{added} - \{OH^-\}_{aq})}{[Glu]_{tot}} \quad (1)$$

(23) Hazen, R. M.; Papineau, D.; Leeker, W. B.; Downs, R. T.; Ferry, J. M.; McCoy, T. J.; Sverjensky, D. A.; Yang, H. X. *Am. Mineral.* **2008**, *93*, 1693–1720.
(24) Köppen, S.; Bronkalla, O.; Langel, W. *J. Phys. Chem. C* **2008**, *112*, 13600–13606.
(25) Brunauer, S.; Emmett, P. H.; Teller, E. *J. Am. Chem. Soc.* **1938**, *60*, 309–319.
(26) Dana, E. S.; Ford, W. E. *Mineralogy*, 4th ed.; John Wiley & Sons, Inc.: New York, 1958.
(27) Sabin, F.; Turk, T.; Vogler, A. *J. Photochem. Photobiol. A* **1992**, *63*(1), 99–106.
(28) Hoffmann, M. R.; Martin, S. T.; Choi, W. Y.; Bahnemann, D. W. *Chem. Rev.* **1995**, *95*, 69–96.
(29) Ryu, J.; Choi, W. *Environ. Sci. Technol.* **2008**, *42*, 294–300.

or, σ_H (μC cm^{-2}) in the H^+-rutile system according to eq 2:

$$\sigma_H = \frac{F \times (([H]_{added} - \{H^+\}_{aq}) - ([OH]_{added} - \{OH^-\}_{aq}))}{A_s \times C_s} \quad (2)$$

in which F is the Faraday constant (96485 C mol^{-1}), A_s is the specific BET surface area (m^2 g^{-1}), and C_s is the solid concentration of particles (g L^{-1}).[30] Potentiometric data from the combined H^+-glutamate-rutile system are presented as μmol of net acid added per m^2 of rutile.

2.2.2. Batch Adsorption Experiments. Batch samples were prepared with a solid concentration of 20 g L^{-1} and a total concentration of L-glutamate ranging from 0.1 to 2 mM (0.3 to 5.6 μmol m^{-2}) in 15 mL Falcon tubes. The pH was adjusted in each sample by adding precise volumes of standardized HCl or NaOH in order to cover the pH range 3−10. pH limits were dictated by the uncertainties in pH measurements of the combination electrode (Thermo-Electron, Orion 8103BNUWP). Argon gas was constantly purged through the suspensions to avoid contamination by CO_2 from air. Preliminary experiments (unpublished data) indicated that the adsorption of glutamate reached a steady state within the first 3 h after addition of glutamate to a rutile suspension. In the batch adsorption experiments presented in this work, samples were put on a test tube rotator (Labroller II, Labnet International, Inc., H5100) at 25 ± 1 °C and 1 bar for 16−20 h to ensure that the adsorption reactions attained a steady state. After this, pH ($-\log\{H^+\}$) was measured using a combination glass electrode that was calibrated in standardized buffers (Fisher Scientific). Samples were centrifuged for 10 min at a relative centrifugal force (RCF) of 1073 xg (Fisher Scientific accuSpin 400) and the concentration of glutamate in the supernatant was measured with UV−vis spectroscopy (Hewlett-Packard, 8452A, Diode Array spectrophotometer) using the ninhydrin-labeling technique.[31−33] In this technique, the amino acid was derivatized by mixing one part of the supernatant with one part HAc-NaAc buffer (pH 5.1) containing 1‰ (w/v) NaCN, and one part ninhydrin 1.5% (w/v) dissolved in 2-methoxyethanol, and heated for 15 min at 100 °C to form a purple complex. After 15 min, ethanol (60%, v/v in H_2O) was added to double the total volume and the vial was cooled in a water bath. When cool, the samples were shaken vigorously for 1 min, left at room temperature for a few minutes, and then analyzed with UV−vis spectroscopy at a wavelength of 570 nm, using a quartz cuvette with a path length of 1 cm. The measured test values were interpreted using the Beer−Lambert law[30] and a molar extinction coefficient (ε) obtained from a calibration curve of known glutamate concentrations. The quantity of glutamate adsorbed at the surface of rutile was calculated as the difference between the known total concentration and the concentration remaining in the aqueous phase after equilibration. Selected supernatants were further analyzed with high performance liquid chromatography (HPLC), showing no sign of degradation of glutamate in solution after being exposed to the rutile mineral.

2.2.3. Efforts Made to Avoid Microbial Contamination. To avoid microbial contamination of the samples, we used sterile Falcon tubes, while laboratory glassware were washed and put in an oven at 500 °C for 8 h prior to use. All solutions and suspensions were freshly prepared prior to each experiment. Also, the reaction times were kept relatively short (maximum of 20 h) to avoid significant growth of microorganism populations. To verify the presence or absence of microorganisms in the batch adsorption samples after reaction, three samples were tested for contamination. An aliquot of each sample was used to inoculate two sterile media (nutrient broth and lysogeny broth). Light microscopy was also used to look for cells. Two samples were found to be sterile, while one was slightly contaminated. However, the two sterile samples returned adsorption results consistent with the slightly contaminated one and therefore we have concluded that microbial contamination did not exert a significant impact on the results observed in this work.

2.3. Surface Complexation Approach. The approach used in the present study builds on the predictive single-site triple-layer model and associated crystal chemical and Born solvation theory referred to as the extended triple-layer model or ETLM.[20,21,34] The calculations reported below were carried out with the computer code GEOSURF described previously.[35] Recent theoretical advances in the application of the ETLM to oxyanion and glutamate adsorption on oxide surfaces have emphasized the role of water dipoles during adsorption and indicated the magnitude of this effect.[4,22,36] These advances have facilitated incorporation of the nature of surface species established by spectroscopic studies into surface complexation calculations. In turn, this modeling has enabled prediction of surface speciation as a function of environmental parameters consistent with spectroscopically established trends. We apply the ETLM here to our data for the glutamate−rutile system in NaCl. We first calibrated the surface protonation and electrolyte adsorption parameters with experimental proton surface titration data for rutile in NaCl solutions. Subsequently, we investigated the applicability of the three surface species deduced previously for glutamate on amorphous titanium dioxide and hydrous ferric oxide.[3−5] In particular, the level of protonation of the surface species is determined from the stoichiometry of the reactions formulated through iterative application of the surface complexation calculations to the experimental adsorption data over a wide range of pH values, ionic strengths, and ligand-to-solid ratios. The results were then tested for consistency with potentiometric titrations of the surface involving the simultaneous presence of glutamate and rutile in NaCl solutions.

3. Results and Discussion

3.1. Titration of Aqueous Glutamate and Rutile , Respectively. The symbols in Figure 2a,b represent experimental titration data of glutamate in aqueous solution in the pH range 3−10 and two NaCl concentrations. This range of conditions covers the de(protonation) steps of the γ-carboxyl and amine group (see Table 1) and serves to check the aqueous speciation model adopted for glutamate, including the effects of glutamate-electrolyte ion-pairing. The overall reproducibility of the experimental data is within ±0.02 mol per mol of glutamate (2%).

The solid lines in Figure 2a,b were calculated theoretically, according to parameters in Table 1. Aqueous protonation of glutamate was treated using equilibrium constants taken from the NIST compilation,[37] and, owing to a lack of information in the literature, electrolyte ion-pairing with glutamate was approximated by assuming that it was the same as literature values for aspartate.[38] This assumption is supported by the calculations described below. Aqueous activity coefficients were calculated using the extended Debye−Hückel equation,[39] using previously described electrolyte characteristics.[40] It can be seen in Figure 2a, b that the calculated lines agree with the experimental data within

(30) Stumm, W.; Morgan, J. J. *Aquatic Chemistry - Chemical Equilibria and Rates in Natural Waters*, 3rd ed.; Wiley-Interscience - John Wiley & Sons, Inc.: New York, 1996.
(31) Lamothe, P. J.; McCormick, P. G. *Anal. Chem.* **1972**, *44*, 821–825.
(32) Friedman, M.; Sigel, C. W. *Biochemistry* **1966**, *5*, 478–485.
(33) McCaldin, D. J. *Chem. Rev.* **1960**, *60*, 39–51.
(34) Sverjensky, D. A. *Geochim. Cosmochim. Acta* **2003**, *67*, 17–28.
(35) Sahai, N.; Sverjensky, D. A. *Comput. Geosci.* **1998**, *24*, 853–873.
(36) Sverjensky, D. A.; Fukushi, K. *Environ. Sci. Technol.* **2006**, *40*, 263–271.
(37) Smith, R. M.; Martell, A. E. *NIST Critically Selected Stability Constants of Metal Complexes Database*; Technology Administration, U.S. Department of Commerce: Washington, DC, 2004.
(38) De Robertis, A.; De Stefano, C.; Gianguzza, A. *Thermochim. Acta* **1991**, *177*, 39–57.
(39) Helgeson, H. C.; Kirkham, D. H.; Flowers, G. C. *Am. J. Sci.* **1981**, *281*, 1249–1516.
(40) Criscenti, L. J.; Sverjensky, D. A. *J. Colloid Interface Sci.* **2002**, *253*, 329–352.

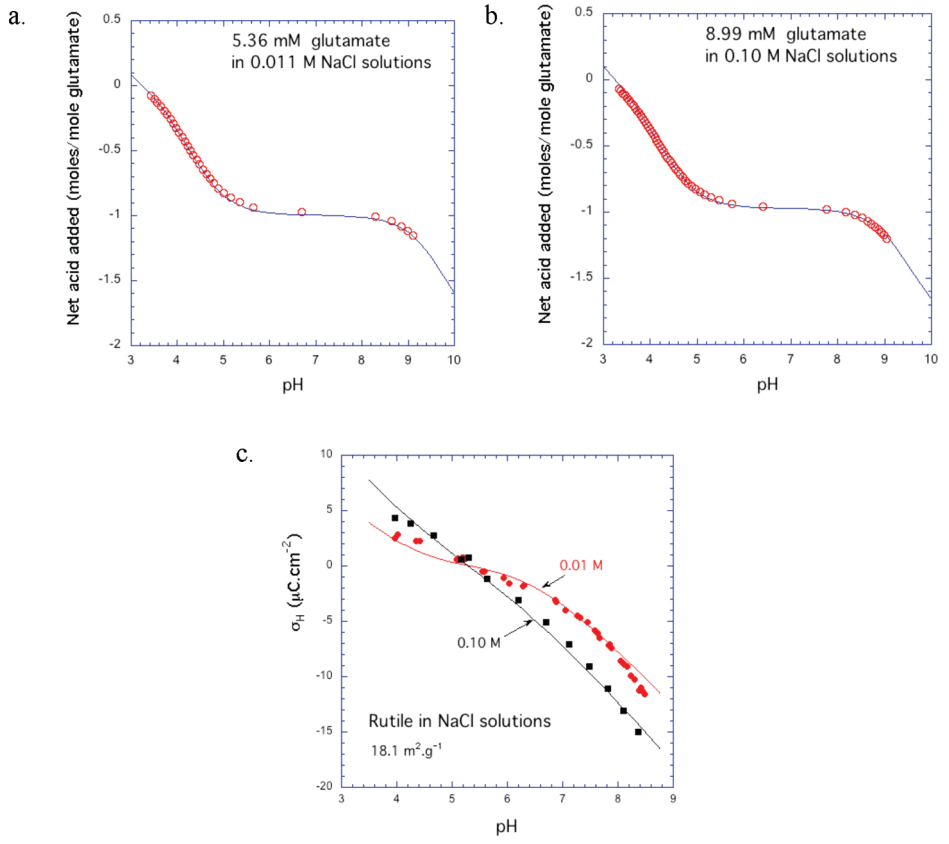

Figure 2. Potentiometric titration data for aqueous glutamate in (a) 0.01 M Na(Cl) and (b) 0.1 M Na(Cl), and for rutile surface (c) in 0.01 and 0.1 M NaCl. Symbols represent experimental data. Solid curves in (a) and (b) were predicted using aqueous glutamate equilibrium constants in Table 1. Solid curves in (c) were calculated using surface protonation and electrolyte adsorption parameters in Table 1.

Table 1. Aqueous Glutamate Properties[a], Rutile (α-TiO_2) Characteristics,[b] and Extended Triple-layer Model Parameters for Proton, Electrolyte, and Glutamate Adsorption on Rutile

reaction type	reaction	log *K*
aqueous glutamate equilibria	$Glu^{2-} + H^+ = HGlu^-$	9.96
	$HGlu^- + H^+ = H_2Glu$	4.30
	$H_2Glu + H^+ = H_3Glu^+$	2.16
	$HGlu^- + Cl^- + 2H^+ = H_3(Glu)Cl$	5.3
	$HGlu^- + Na^+ = Na(HGlu)$	−0.3
	$HGlu^- + Na^+ = NaGlu^- + H^+$	−9.6
surface equilibria	hypothetical 1.0 m standard state	
$\log K_1^0$	$>TiOH + H^+ = >TiOH_2^+$	2.52
$\log K_2^0$	$>TiO^- + H^+ = >TiOH$	8.28
$\log {}^*K^0_{Na^+}$	$>TiOH + Na^+ = >TiO^-\_Na^+ + H^+$	−5.6
$\log {}^*K^0_{Cl^-}$	$>TiOH + H^+ + Cl^- = >TiOH_2^+\_Cl^-$	5.0
$\log {}^*K^0_{>Ti_2(>TiOH)_2Glu}$	$4>TiOH + H^+ + HGlu^- = >Ti_2(>TiOH)_2Glu + 2H_2O$	16.2
$\log {}^*K^0_{>Ti(OH_2^+)Glu^-}$	$>Ti(OH)_2 + H^+ + HGlu^- = >Ti(OH_2^+)Glu^- + H_2O$	8.1
surface equilibria	site-occupancy standard states[c]	
$\log K^\theta_{>Ti_2(>TiOH)_2Glu}$	$2>TiOH_2^+ + 2>TiOH + HGlu^- = >Ti_2(>TiOH)_2Glu + H^+ + 2H_2O$	20.5
$\log K^\theta_{>Ti(OH_2^+)Glu^-}$	$>Ti(OH_2^+)_2 + HGlu^- = >Ti(OH_2^+)Glu^- + H^+ + H_2O$	5.6

[a] Protonation constants from Smith and Martell (2004);[37] electrolyte ion pair constants assumed to be the same as for aspartate given by De Robertis and De Stefano (1991).[38] [b] Rutile properties are $N_s = 3.0$ sites nm^{-2}, $A_s = 18.1\ m^2\ g^{-1}$, $C_1 = 120\ \mu F\ cm^{-2}$, $C_2 = 120\ \mu F\ cm^{-2}$, $pH_{PPZC} = 5.4$, $\Delta pK_n^\theta = 6.3$, $\log K_1^\theta = 5.25$, $\log K_2^\theta = 8.50$, $\log K^\theta_{Na^+} = 2.68$, $\log K^\theta_{Cl^-} = 2.48$ (see text). [c] Equilibrium constants relative to site-occupancy standard states were also written relative to charged surface sites calculated using the equations:

$$\log K^\theta_{>Ti_2(>TiOH)_2Glu} = \log {}^*K^0_{>Ti_2(>TiOH)_2Glu} + \log \frac{(N_sA_S)^4C_s^3}{100} - 2pH_{PPZC} + \Delta pK_n^\theta$$

$$\log K^\theta_{>Ti(OH_2^+)Glu^-} = \log {}^*K^0_{>Ti(OH_2^+)Glu^-} + \log \frac{(N_sA_S)}{100} - pH_{PPZC} + \frac{\Delta pK_n^\theta}{2}$$

where N_s is site density (sites nm^{-2}), A_s is BET surface area ($m^2\ g^{-1}$), and C_s is solid concentration ($g\ L^{-1}$).

the estimated experimental uncertainty. Also, varying the background electrolyte concentration from 0.01 to 0.1 M NaCl does not significantly change the (de)protonation behavior of glutamate, as Figure 2a,b are nearly indistinguishable.

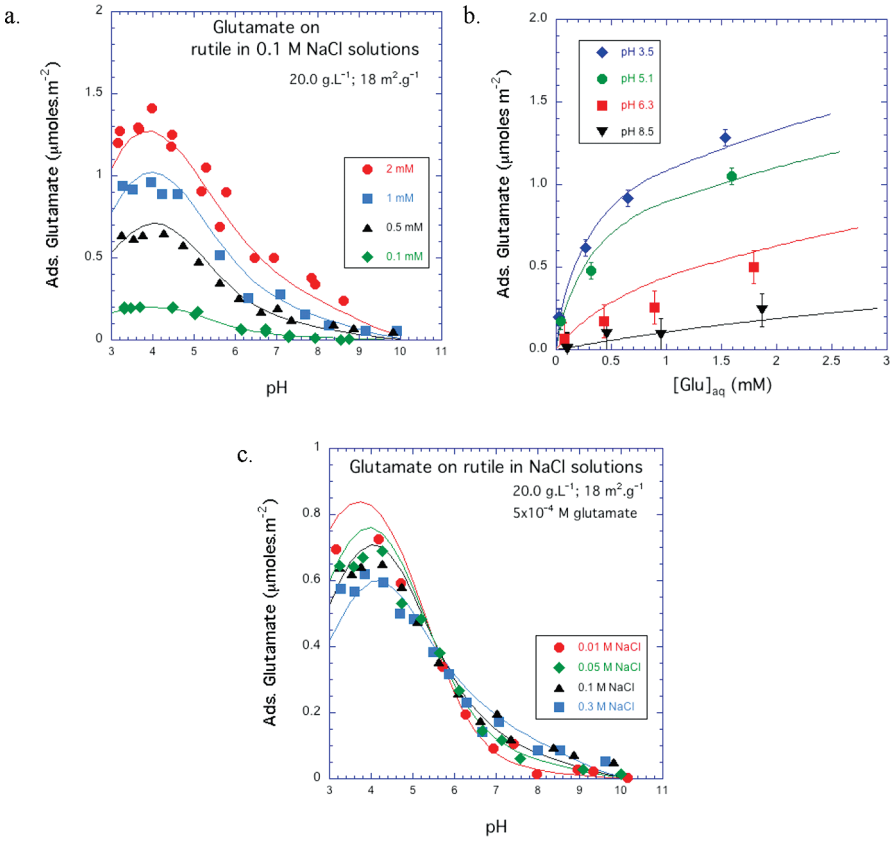

Figure 3. Adsorption of glutamate on rutile as a function of environmental conditions. Symbols represent experimental data from batch adsorption experiments, visualized as (a) μmol of Glu adsorbed per m^2 vs pH in 0.1 M Na(Cl); (b) μmol of Glu adsorbed per m^2 vs $[Glu]_{aq}$ in 0.1 M Na(Cl); (c) μmol of Glu adsorbed per m^2 vs pH at 0.01, 0.05, 0.1, and 0.3 M Na(Cl), respectively. The estimated experimental uncertainty might be a maximum of ± 0.1 μmol m^{-2}. Solid curves were calculated using the glutamate adsorption model with parameters in Table 1.

The (de)protonation reactions of the rutile surface were studied with potentiometric titrations in the pH range 4−9 and at two NaCl concentrations (Figure 2c). The intersection of the titration data defines the point of zero salt effect ($pH_{PZSE} = 5.37$) of rutile in NaCl solutions. This value can be used to estimate the pristine point of zero charge (pH_{PPZC}) with the relation

$$pH_{PPZC} = pH_{PZSE} + 0.5(\log K^{\theta}_{Cl^-} - \log K^{\theta}_{Na^+}) \qquad (3)$$

using theoretical estimates of $\log K^{\theta}_{Na^+}$ and $\log K^{\theta}_{Cl^-}$ published previously.[20] The resulting pH_{PPZC} of 5.4 (± 0.1) coincides with the $pH_{PPZC} = 5.4$ obtained by Machesky et al.,[14] using a similarly prepared rutile. The solid lines in Figure 2c were calculated theoretically using the protonation and electrolyte adsorption equilibrium constants, capacitances, and the site density in Table 1. Only the electrolyte adsorption equilibrium constants and the capacitance C_1 were varied to fit the data. Because the two electrolyte equilibrium constants are related by the pH_{PZSE}, this results in a two-parameter fit to the data. Estimated uncertainties in these parameters are ± 0.2 in the log K values and ± 10 μF cm^{-2} for the capacitance. The two protonation constants were calculated from the pH_{PPZC} and a theoretical value of ΔpK^{θ}_n from ref 20.[20] The value of C_2 is set equal to that of C_1 in the ETLM.[20,22] The site density in Table 1 was established during regression of the glutamate adsorption data discussed next. It can be seen in Figure 2c that, despite minor deviations from the trends of the data at the extremes of pH, the curves in Figure 2c agree with the experimental data within an estimated experimental uncertainty of ± 0.3 μC cm^{-2}, based on reproducibility.

3.2. Adsorption of Glutamate on Rutile. Adsorption data for L-glutamate on rutile in 0.1 M Na(Cl) are shown in Figure 3a. The total concentration of glutamate ranged from 0.1 to 2 mM (0.3−5.6 μmol m^{-2}). In all cases, the largest amount of glutamate was adsorbed around pH 4. At this pH, about 40% of the aqueous glutamate has a net negative charge, which favors adsorption to the positively charged rutile surface. The adsorption decreases at higher pH, which reflects the unfavorable electrostatic conditions above the pH_{PPZC} (5.4) of rutile for a negatively charged glutamate molecule to adsorb to a negatively charged surface. Below pH 4, where rutile is mainly positively charged, glutamate exists predominantly in a net neutral form in aqueous solution leading to a small decrease in adsorption. However, it should also be noted that small but significant amounts of adsorption occur at pH values between 6 and 9, an indication that the adsorption is not driven by electrostatic factors alone (see also ref 5).

A selection of data points from Figure 3a has been reorganized in Figure 3b to illustrate the amount of adsorbed glutamate on rutile as a function of aqueous glutamate concentration in 0.1 M Na(Cl). Symbols in Figure 3b represent the adsorption of glutamate at pH 3.5, 5.1, 6.3, and 8.5, respectively. From this figure it is clear that the highest amount of adsorbed glutamate occurs at low pH. The adsorption trends do not reach an observable plateau with increased aqueous glutamate concentration, indicating that a saturation of available sites on the rutile surface has not yet been attained. However, in the experiments we used the difference between the total concentration of glutamate and the concentration remaining in solution to quantify adsorption, and since the removal of glutamate from solution is only

20% or less at our highest ligand-to-solid ratio, it is difficult to increase the ligand-to-solid ratio further and still get reliable results. Under these conditions (circles in Figure 3a), the estimated experimental uncertainty might be a maximum of ±0.1 μmol m^{-2}.

In order to evaluate whether the adsorption of glutamate on rutile is dependent on ionic strength, batch adsorption experiments were performed at different background electrolyte concentrations, as shown in Figure 3c. Na(Cl) concentrations used were 0.01, 0.05, 0.1, and 0.3 M, respectively, while the total concentration of glutamate was kept constant at 0.5 mM (1.4 μmol m^{-2}) in all experiments. Data at 3 < pH < 5, which is the interval where glutamate adsorbs to the highest extent, indicate an ionic strength dependence. The lowest electrolyte concentration (0.01 M) yields the highest amount of adsorption. This is followed by a decrease in adsorption at gradually higher NaCl concentrations. On average, the difference in glutamate adsorption between highest and lowest electrolyte concentrations at 3 < pH < 5 is 0.15 μmol m^{-2}, which corresponds to a 20% difference in total amount of adsorbed glutamate. Between pH 5 and 6.5 there is no significant dispersion of the data. Some ionic strength dependence might exist at above pH 6.5, although opposite trends are observed compared to low pH values. However, because of the low amount of adsorbed glutamate at these high pH values, the relative uncertainty of the results are higher and it is difficult to draw reliable conclusions about a possible ionic strength dependence in this region from the data alone.

Two surface complexation reactions, corresponding to the formation of the species depicted in Figure 4a,b, were found to be consistent with the adsorption data plotted in Figure 3. The two species depicted in Figure 4a,b represent two of the three coordination modes previously inferred from ATR-FTIR spectroscopic studies of glutamate on amorphous titanium dioxide.[5] The reactions are represented as follows:

Bridging-bidentate species (Figure 4a)

$$4{>}\mathrm{TiOH}+\mathrm{H^+}+\mathrm{HGlu^-}={>}\mathrm{Ti_2}({>}\mathrm{TiOH})_2\mathrm{Glu}+2\mathrm{H_2O} \quad (4)$$

Chelating species (Figure 4b)

$${>}\mathrm{Ti(OH)_2}+\mathrm{H^+}+\mathrm{HGlu^-}={>}\mathrm{Ti(OH_2^+)Glu^-}+\mathrm{H_2O} \quad (5)$$

>TiOH groups that participate in surface protonation reactions in water occur on all the major crystal faces indicated in Figure 1.[16,41,42] >Ti(OH)$_2$ groups occur on the (111) plane indicated in Figure 1.[41] Representation of such groups in the context of a single-site model has been done previously.[43]

It can be seen in Figure 4a,b that both species can be thought of as partly inner-sphere and partly hydrogen bonded. The bridging-bidentate species >Ti$_2$(>TiOH)$_2$Glu (Figure 4a) has four points of attachment of the glutamate to the surface, two of which are inner-sphere and two of which are hydrogen bonded; that is, the glutamate molecule can be thought of as "lying down" on the surface. Both carboxylate groups are coordinated to the surface in the same way: one O is coordinated directly to a Ti by a Ti−O−C bond, and the other is coordinated through a hydrogen bond to a different Ti, that is, TiOH···O=C. This species has the same

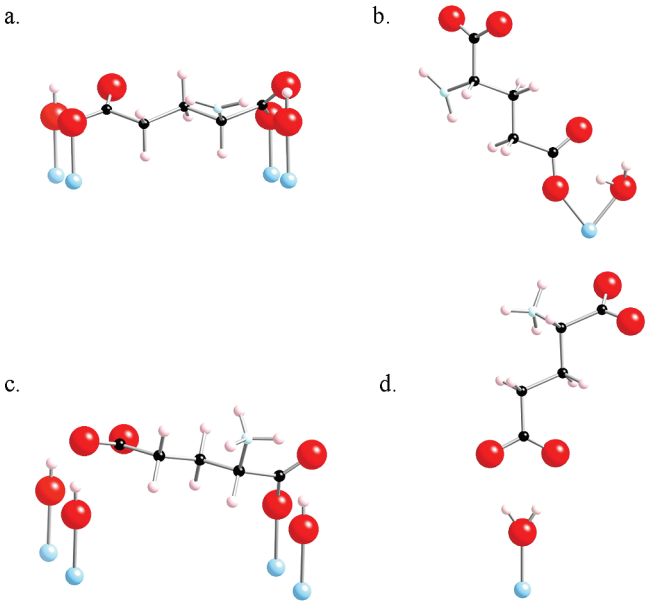

Figure 4. Possible surface species representing different modes of attachment of glutamate to rutile surface sites, consistent with the surface complexation calculations in the present study. Large spheres indicate oxygen atoms, small filled spheres carbon, small pale spheres hydrogen or nitrogen, and the lowermost spheres titanium at the rutile surface. (a) Bridging-bidentate species with four points of attachment involving one inner-sphere Ti−O−C bond and one Ti−OH···O=C hydrogen bond for each carboxylate (eq 4). (b) Chelating species with two points of attachment involving one inner-sphere Ti−O−C bond and one Ti−OH$_2^+$···O=C to a single titanium (eq 5). (c) Alternative to the bridging-bidentate species in (a). This bridging-bidentate species has four points of attachment involving one inner-sphere Ti−O−C bond and one Ti−OH···O=C hydrogen bond of the α-carboxylate, and one Ti−OH···$^-$O−C hydrogen bond and one Ti−OH···O=C hydrogen bond of the γ-carboxylate (stabilized through resonance) (eq 6). (d) Alternative to the chelating species in (b), outer-sphere or hydrogen bonded to the surface (eq 7).

stoichiometry as one previously inferred for amorphous titanium dioxide and HFO.[4,5]

The chelating species >Ti(OH$_2^+$)Glu$^-$ (Figure 4b) has two points of attachment, the γ-carboxylate chelates to a single Ti with one Ti−O−C bond and one TiOH$_2^+$···O=C hydrogen bond. The α-carboxylate and amine groups are pointing away from the surface, that is, the glutamate molecule is "standing up" on the surface. This species is very similar to the chelating species previously inferred but includes an extra proton on the >Ti(OH$_2^+$) group. On the basis of our previous study,[4] it is expected that the bridging-bidentate species will be the predominant one at low surface coverages, whereas the chelating species will predominate at high surface coverages.

It should also be noted that the reactions in eqs 4 and 5 are computationally almost identical to the reactions

$$4{>}\mathrm{TiOH}+\mathrm{H^+}+\mathrm{HGlu^-}={>}\mathrm{Ti}({>}\mathrm{TiOH})_3\mathrm{HGlu}+\mathrm{H_2O} \quad (6)$$

and

$${>}\mathrm{TiOH}+\mathrm{H^+}+\mathrm{HGlu^-}={>}\mathrm{TiOH_2^+}\_\mathrm{HGlu^-} \quad (7)$$

respectively. Equations 4 and 5 refer to the completely deprotonated form of glutamate. This is similar to results for many inorganic and organic oxyanions which adsorb as partially or

(41) Koretsky, C. M.; Sverjensky, D. A.; Sahai, N. *Am. J. Sci.* **1998**, *298*, 349–438.
(42) Dobson, K. D.; Connor, P. A.; McQuillan, A. J. *Langmuir* **1997**, *13*, 2614–2616.
(43) Arai, Y.; Sparks, D. L.; Davis, J. A. *Environ. Sci. Technol.* **2004**, *38*, 817–824.

completely deprotonated species at pH values where the aqueous oxyanion is protonated.[44−48] However, eqs 6 and 7 refer to the glutamate with the amine group protonated. The two surface glutamate species in eqs 6 and 7 are depicted in Figure 4, panels c and d, respectively. The surface species $>\mathrm{Ti}(>\mathrm{TiOH})_3\mathrm{HGlu}$ in eq 6 may still be thought of as representing four points of attachment. However, there is only one inner-sphere Ti−O−C bond and one Ti−OH···O═C bond of the α-carboxylate, and one Ti−OH···$^{-}$O−C hydrogen bond and one Ti−OH···O═C bond of the γ-carboxylate (stabilized through resonance). In contrast, the surface species in eq 7, $>\mathrm{TiOH_2}^{+}\_\mathrm{HGlu}^{-}$, may represent an outer-sphere and/or hydrogen bonded species. We emphasize that the two species in Figure 4c,d represent alternatives to the species in Figure 4a,b. Our surface complexation model cannot distinguish between the species in Figure 4a,b relative to Figure 4c,d. Spectroscopic measurements and molecular calculations may help to distinguish between these possibilities. In the present study, we depict the surface species using the reactions in eqs 4 and 5 because they are closest to the types of surface species suggested by the ATR-FTIR spectroscopic study of amorphous titanium dioxide.[5] In any case, it should be emphasized that it is primarily the reaction stoichiometries being established here by the surface complexation model.

The reactions in eqs 4 and 5 correspond to the equilibrium constants

$$\log^{*} K^{0}_{>\mathrm{Ti_2(>TiOH)_2Glu}} = \frac{a_{>\mathrm{Ti_2(>TiOH)_2Glu}} a^{2}_{\mathrm{H_2O}}}{a^{4}_{>\mathrm{TiOH}} a_{\mathrm{H^+}} a_{\mathrm{HGlu^-}}} 10^{F\Delta\psi_{r,4}/2.303RT} \quad (8)$$

and

$$\log^{*} K^{0}_{>\mathrm{Ti(OH_2^+)Glu^-}} = \frac{a_{>\mathrm{Ti(OH_2^+)Glu^-}} a_{\mathrm{H_2O}}}{a_{>\mathrm{Ti(OH)_2}} a_{\mathrm{H^+}} a_{\mathrm{HGlu^-}}} 10^{F\Delta\psi_{r,5}/2.303RT} \quad (9)$$

where the superscripts "*" and "0" refer to reactions written relative to >TiOH, and to the hypothetical 1.0 M standard states, respectively.[34] The terms involving $\Delta\psi_{r,4}$ and $\Delta\psi_{r,5}$ in eqs 8 and 9 represent the electrical work involved in the reaction. In the ETLM, the electrical work includes contributions not only for the ions going on or off the surface, but also for the water dipoles coming off the surface in eqs 4 and 5. The latter contribution to $\Delta\psi_r$ is $-n_{\mathrm{H_2O}}(\psi_0 - \psi_\beta)$, where $n_{\mathrm{H_2O}}$ represents the number of moles of water on the right-hand side of the reaction. In eqs 4 and 5, $n_{\mathrm{H_2O}} = 2$ and 1, respectively, which results in $\Delta\psi_{r,4} = 0$ and $\Delta\psi_{r,5} = \psi_0 - \psi_\beta$. In eqs 6 and 7, $\Delta\psi_{r,6} = 0$ and $\Delta\psi_{r,7} = \psi_0 - \psi_\beta$, the same overall result as for eqs 4 and 5.

The solid curves in Figure 3 represent regression calculations using the reactions in eqs 4 and 5. On the basis of the estimated experimental uncertainties and the uncertainties in the regression parameters discussed above, the calculated curves in the figures show relatively small discrepancies with the experimental data. Clearly, the two reactions are sufficient to describe glutamate adsorption on rutile as a function of pH, ligand-to-solid ratio, and ionic strength. The two glutamate surface species involved represent two of the three coordination modes for glutamate on amorphous titanium dioxide indicated by ATR-FTIR spectroscopy.[5] The third coordination mode was represented by a chelating-monodentate species, which was previously treated in our surface complexation model for HFO as $>\mathrm{Fe}>\mathrm{Fe(OH_2^+)Glu}$.[4] It is interesting to note that the chelating-monodentate species for rutile (i.e., $>\mathrm{Ti}>\mathrm{Ti(OH_2^+)Glu}$) together with the chelating species used above (eq 5) can also describe the adsorption data in Figure 3. However, this alternate pair of species does not predict the experimentally observed decrease of the isoelectric point with increased glutamate concentration.[7] The positive charge on the species $>\mathrm{Ti}>\mathrm{Ti(OH_2^+)Glu}$ results in a predicted increase in the isoelectric point with glutamate concentration. In contrast, the bridging-bidentate and chelating pair in reactions 4 and 5 do result in prediction of a strong decrease in the isoelectric point. For example, for the highest glutamate concentration in Figure 3a, the isoelectric point is predicted to be 4.3 from model values of the potential on the d-plane of the triple layer model. This value is a substantial decrease from 5.4 without glutamate present. The decrease of 1.1 pH units is similar to the decrease of 1.7 pH units obtained for rutile in 2 mM glutamate as reported by Fuerstenau et al.[7] However, a direct comparison of the two values is not possible, since Fuerstenau et al. did not report the solid concentration of rutile in their experiments.

The regression calculations discussed above generated values of the equilibrium constants for glutamate adsorption represented by $\log^{*}K^{0}_{>\mathrm{Ti_2(>TiOH)_2Glu}}$ and $\log^{*}K^{0}_{>\mathrm{Ti(OH_2^+)Glu^-}}$ and the site density (N_s) in Table 1. Estimated uncertainties are ±0.2 in the log K values and ±0.5 in the site density. As stated above, these equilibrium constants refer to the hypothetical 1.0 M standard state.[34] They were converted to values of $\log K^{\theta}_{>\mathrm{Ti_2(>TiOH)_2Glu}}$ and $\log K^{\theta}_{>\mathrm{Ti(OH_2^+)Glu^-}}$, where the "$\theta$" refers to site-occupancy standard states, and referenced to $>\mathrm{TiO^-}$ using equations and the values of N_s (site density), A_s (BET surface area), C_s (solid concentration), $\mathrm{pH_{PPZC}}$, and $\Delta\ \mathrm{p}K^{\theta}_{n}$ given in Table 1. The values of $\log K^{\theta}_{j}$ for the jth species in Table 1 are independent of the individual sample characteristics. Consequently, values of $\log K^{\theta}_{j}$ are useful for comparing the binding of glutamate on different oxides. Furthermore, the high dielectric constant of rutile[20] enables the use of these $\log K^{\theta}_{j}$ values in the application of Born solvation theory to prediction of equilibrium constants for glutamate adsorption on other solids with lower dielectric constants.[20−22] Our equilibrium constants for glutamate adsorption were tested by predicting the proton uptake for the combined glutamate−rutile system followed by a comparison with the corresponding experimental titration data.

3.3. Titration of Glutamate on Rutile. Potentiometric titrations of rutile in 0.1 M Na(Cl) with various concentrations of glutamate present are represented by the symbols in Figure 5. Data are given as μmol of net protons added per m^2 of rutile. Consequently, each data point represents the sum of protons involved in aqueous glutamate protonation, surface protonation, and electrolyte adsorption on rutile, and glutamate adsorption. Between pH values of about 7 and 9, the data primarily represent protons involved in aqueous glutamate protonation and surface protonation and electrolyte adsorption, since only a maximum of 0.5 μmol of glutamate is adsorbed per m^2 (15% of the total concentration of glutamate) under these conditions (Figure 3a). Glutamate adsorbs most strongly at about pH 4. Consequently, between pH values of about 4 and 6, the data represent protons involved in glutamate adsorption as well as protons involved in surface protonation and electrolyte adsorption (see reactions in Table 1 and calculated percentages of glutamate surface species in Figure 6). The solid curves in Figure 5 represent predictions using the model discussed above. The close fit of the solid curves to the

(44) Arai, Y.; Elzinga, E. J.; Sparks, D. L. *J. Colloid Interface Sci.* **2001**, *235*, 80–88.
(45) Arai, Y.; Sparks, D. L. *J. Colloid Interface Sci.* **2001**, *241*, 317–326.
(46) Peak, D.; Luther, G. W.; Sparks, D. L. *Geochim. Cosmochim. Acta* **2003**, *67*, 2551–2560.
(47) Persson, P.; Axe, K. *Geochim. Cosmochim. Acta* **2005**, *69*, 541–552.
(48) Hwang, Y. S.; Liu, J.; Lenhart, J. J.; Hadad, C. M. *J. Colloid Interface Sci.* **2007**, *307*, 124–134.

experimental data in the pH range of about 4−6 strongly supports the validity of the proton stoichiometry of the adsorption reactions in eqs 4 and 5.

3.4. Prediction of Glutamate Surface Speciation. The predicted surface speciation of glutamate as a function of pH, ligand-to-solid ratio, and ionic strength is shown in Figure 6a−d. It can be seen in these figures that the predicted proportions of the two surface glutamate species vary strongly with environmental conditions. Similar variations were inferred for the surface speciation of glutamate on amorphous titanium dioxide.[5] However, the number of species and the details of the reaction stoichiometries for glutamate on rutile inferred in the present study differ from those inferred for amorphous titanium dioxide and hydrous ferric oxide in our previous study.[4] As discussed above, in the present study we found that only two reaction stoichiometries were needed instead of three and that an extra proton was required in the reaction for the chelating species.

It can be seen that the chelating species is predicted to have a maximum in concentration at pH values of about 4−6, depending on the ionic strength and the total glutamate concentration. It is interesting to note that this maximum in the abundance of the chelating species is approximately coincident with the pK = 4.3 for the γ-carboxylate group of the aqueous glutamate. However, the bridging-bidentate species concentration is unimportant above pH 6 and increases steadily at progressively lower pH values.

The bridging-bidentate species is at its maximum importance at the lowest pH values, the lowest total glutamate concentration, and the highest ionic strength, under which conditions it can be the predominant surface complex of glutamate on rutile (Figure 6a,d). Under all other conditions, the predominant surface species of glutamate is the chelating species. With increases in ionic strength, the bridging-bidentate adsorption is mildly affected, whereas the chelating species adsorption is diminished and broadened with respect to pH.

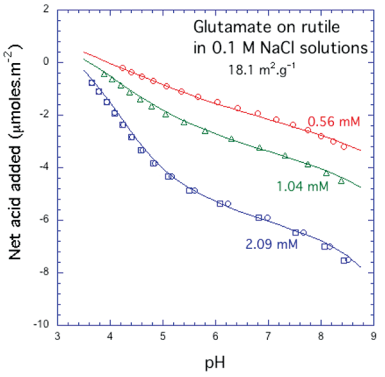

Figure 5. Potentiometric titrations of rutile in 0.1 M NaCl in the presence of glutamate. Symbols represent experimental data. Solid curves were predicted using the glutamate adsorption model fitted to the data in Figures 2 and 3.

4. Conclusions

Potentiometric titrations and batch adsorption experiments were performed over a wide range of environmental conditions at 25 °C and 1 bar to study the adsorption of L-glutamate on the surface of well-characterized rutile. Results show that rutile surface (de)protonation reactions are dependent on the

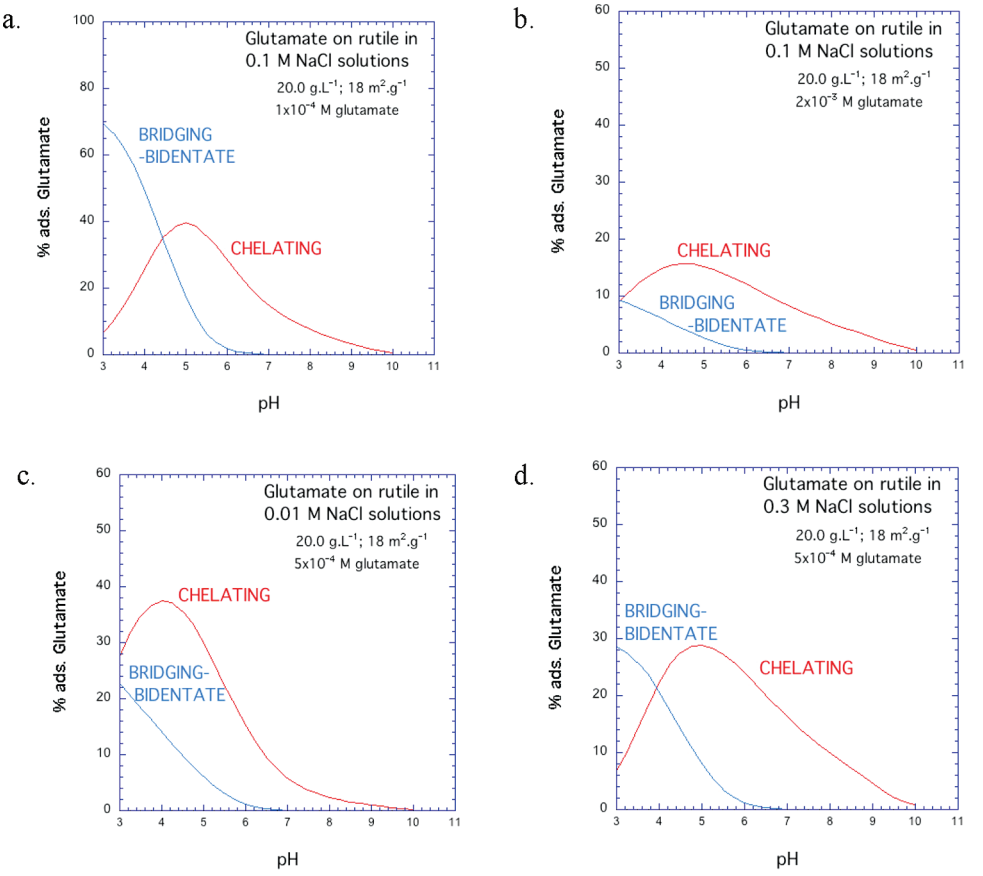

Figure 6. Predicted surface speciation of glutamate on rutile as a function of environmental conditions. The species names refer to the pictures in Figure 4 and the reaction stoichiometries in eqs 4 and 5.

background NaCl concentration, and the mineral powder has a pH_{PPZC} of 5.4. Adsorption of glutamate on rutile is favored at pH < 5. The decrease in adsorption at higher pH reflects the unfavorable electrostatic conditions for a negatively charged glutamate molecule to adsorb to a negatively charged surface. Further, glutamate adsorption on rutile shows ionic strength dependence, especially at low pH. An extended triple-layer surface complexation model of these experimental results indicates the possible existence of at least two surface complexes. One possible pair of complexes involves a bridging-bidentate species binding through both carboxyl groups, which can be thought of as "lying down" on the surface (as found previously for amorphous titanium dioxide and hydrous ferric oxide), together with a chelating species which binds only through the γ-carboxyl group, that is, "standing up" at the surface. The calculated proportions of these two surface glutamate species vary strongly with environmental conditions. The use of complementary techniques provides an extended comprehension of glutamate−rutile interactions, and by predicting speciation, surface complexation models give us a more complete understanding of the behavior of amino acids in different environments.

Acknowledgment. The authors are extremely grateful for the specially cleaned rutile powder sample provided to them by J. Rosenqvist and D. Wesolowski of the Oak Ridge National Laboratory, as well as M. Machesky. We greatly appreciate discussions with G. D. Cody, J. A. Davis, P. Fenter, A. J. McQuillan, J. Rosenqvist, and D. L. Sparks. We thank C. Hadidiacos and T. Kuribayashi for their assistance during SEM and XRD measurements, respectively. P. Griffin is gratefully acknowledged for performing tests for microbial contamination. We also wish to thank N. Lee and C. Estrada for help in the laboratory and discussions. Financial support was provided by a joint National Science Foundation - NASA Astrobiology Institute Collaborative Research Grant to the Johns Hopkins University and the Carnegie Institution for Science. D.A.S., C.M.J., and C.L.J. would like to express their appreciation for the facilities and hospitality extended to them by the Geophysical Laboratory of the Carnegie Institution of Washington.

Supporting Information Available: Tables showing data from batch adsorption experiments as a function of environmental conditions (Figure 3). This information is available free of charge via the Internet at http://pubs.acs.org.